ACS Sustainable Chemistry & Engineering

Research Article

pubs.acs.org/journal/ascecg

Development of Coconut Shell Activated Carbon-Tethered Urease for Degradation of Urea in a Packed Bed

Lei Wang, Sha Wang, Xiangyun Deng, Yucang Zhang, and Chunrong Xiong*

Key Lab of Ministry of Education for Advanced Materials of Tropical Island Resources, Hainan University, Haikou 570228, P. R. China

Supporting Information

ABSTRACT: Coconut shell activated carbon (AC)-tethered urease (from jack bean) was successfully developed to degrade urea in a packed bed reactor. The loading capacity of urease in AC was 78.8 mg/g. The tethered enzyme showed a maximum activity at 70 °C and pH 7.2. For higher than 75% of the maximum activity, the tethered urease showed a broader temperature range of 42−80 °C compared to 45−75 °C for the free enzyme. Similarly, the tethered urease had an increased stability against the changes of pH. The K_m value of the free urease was 0.271 mol/L and 0.345 mol/L for the tethered one. This may be caused by the conformational changes of the enzyme. The V_{max} values were 0.215 and 0.110 mol/min for the tethered and free ureases, respectively, which is reflected by an increase in catalytic activity. The catalytic degradation of urea was performed in a packed bed reactor. The remaining activity of the tethered urease was over 80% after 50 h of operation.

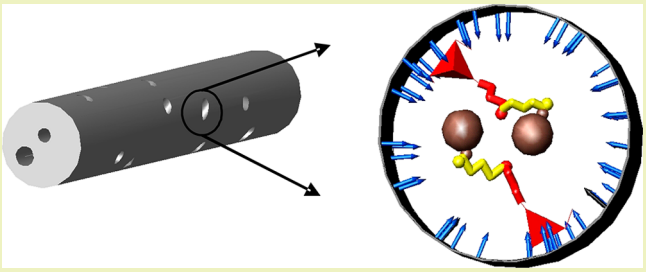

KEYWORDS: *Coconut shell activated carbon, Urease, Degradation of urea, Immobilization, Packed bed reactor*

INTRODUCTION

The removal of urea from aqueous solutions is a major problem in various industries due to increased environmental and health concerns. The production of urea has reached about 10^8 tons per year worldwide.[1] In production, urea-containing (0.2−2%) wastewater mainly results from the urea purification and recovery process. In the environment, urea also comes from other industries that utilize urea, as well as from fertilized crop-planted soils and urine excretion by animals. Although urea has low ecotoxicity, the long-term impact in nature may cause eutrophication and groundwater pollution.

Urea is a polar nonionic compound, showing little affinity to common sorbents.[2] It is highly soluble and stable in water. The industrially utilized method to remove urea is based on nonenzymatic hydrolysis, which requires high temperature and high pressure in addition to complex technological equipments. Other urea removal methods include catalytic and electrochemical decompositions, oxidation with strong oxidants, and adsorption, which have high operation costs.[1−3] Ureases are a group of highly prominent enzymes, widely distributed in nature. They can catalyze the hydrolysis of urea to carbonic acid and ammonia. Therefore, the hydrolysis of urea catalyzed by urease is a "green" route.

Immobilized enzymes can be easily removed from the reaction medium and can be operated in batch or continuous processes.[4] Immobilization of enzymes might avoid some inactivation caused by aggregation, proteolysis, or interaction with external interfaces. Meanwhile, it can improve its stability, activity, selectivity, and reduce inhibitions.[5] A variety of solids have been studied for the immobilization of enzymes. Some studies have concluded that organic carriers have some disadvantages including susceptibility to microbial attack, shrinkage of pore sizes with variations of pH, solvent composition, and flow rate in column reactors.[6] Comparatively, most inorganic carriers are inert and stable at high temperatures. Their surface can be easily functionalized for binding moieties. Moreover, enzymes can be accommodated in their pores.[7] Among inorganic carriers,[8−14] mesoporous silicas, such as MCM-41, SBA-15, etc., have been the focus of a number of studies because of their large surface area, high pore volume, and opened structure.[15,16] Although they have been widely researched to immobilize enzymea in order to facilitate catalyst recycling, they are not applicable in a packed bed reactor. Mesoporous silica-supported enzymes are powdery substances. To be processed into macro-sized granules, silica powder is normally mixed with an adhesive binder and subjected to annealing at high temperature. However, enzymes cannot stand a high temperature. Therefore, their catalytic performances are limited to a slurry reactor, and catalysts must be separated after each run.

Kibarer et al.[17] studied the physical adsorption of urease in petroleum-based activated charcoal, which has been coated with hexamethyldisiloxane through plasma polymerization. George et al.[18] immobilized crude urease onto polyester. Moynihan et al.[19] reported urea hydrolysis by the immobilized urease onto ion exchange resins in a fixed-bed reactor. Comparatively,

Received: September 5, 2013
Revised: December 7, 2013
Published: December 11, 2013

 © 2013 American Chemical Society

coconut shell AC, a biomass based material, has high mechanical strength, good abrasion resistance, and inherent granular structure, making it applicable to a continuous packed bed. In addition, the pore sizes of AC are more tunable in a range from 5 to 50 nm by simply controlling the preparation conditions. It is fairly suitable for proper immobilization of high molecular weight enzymes and the diffusion of substrate and product through the pore channel.[20−23] In this paper, coconut shell AC granules were controllably oxidized to generate abundant phenolic groups on the surface, followed by aminosilylation and glutaraldehyde linking to tether the urease. The urease is also a kind of multimeric protein, the same as many other enzymes. It is possible to reach some multipoint covalent attachment using glutaraldehyde.[5] The immobilized urease can be applied to remove urea in a packed bed reactor.

EXPERIMENTAL SECTION

Materials. The jack bean urease (EC 3.5.1.5, molecular weight about 480 kDa, 50,000−100,000 units/g) and (3-aminopropyl)-trimethoxysilane (APTMS, 97%) were purchased from Sigma Chemical Co. Coconut shell activated carbon granules (20−40 mesh, specific gravity 1.8) and glutaraldehyde (50% aqueous solution) were obtained from Aladdin reagent Co. (Shanghai, China). HNO_3, HCl, NaOH, $NaHCO_3$, and Na_2CO_3 were purchased from Sinopharm Chemical Reagent Co. (China). Quartz granules (1−20 mesh) were obtained from Guangzhou Chemical Reagent Co. (China).

Functionalization of Coconut Shell AC. Coconut shell AC granules were successively subjected to oxidation, aminosilylation, and aldehyde linking prior to urease immobilization, which is presented in Figure 1. Coconut shell AC granules were placed into a Soxhlet

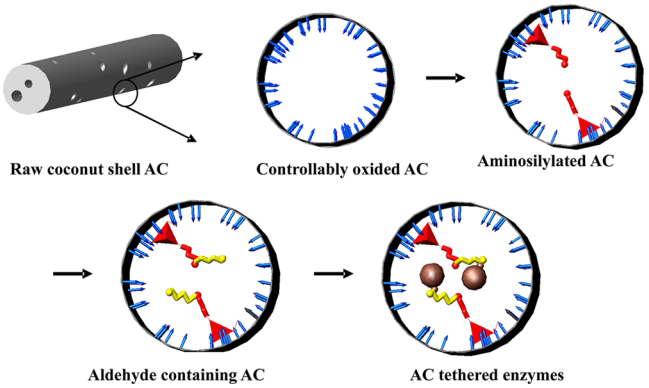

Figure 1. Process of enzyme immobilization in coconut shell AC granules.

extractor and washed with deionized water at 100 °C for 12 h, and then dried at 105 °C for 24 h. Five grams of AC granules were oxidized with 50 mL of 20 wt % HNO_3 in a reflux device at 80 °C for 3 h. The oxidized AC granules were thoroughly washed with distilled water and then dried at 105 °C for 24 h.

To aminosilylate the oxidized AC, 3 g of oxidized AC and 2 mL of APTMS (97%) were stirred in 80 mL toluene under reflux for 12 h. The solid was separated by suction filtration, and then washed successively with dichloromethane and ethanol. The physically adsorbed APTMS in the AC was extracted with ethanol in a Soxhlet extractor for 24 h. The surface of the aminosilylated coconut shell AC was further modified with aldehyde groups by reacting with glutaraldehyde.[10] Three grams of aminosilylated AC was stirred with 5 mL of 50% aqueous glutaraldehyde in 50 mL ethanol solution under reflux for 2 h. The solid was separated by suction filtration, and then followed by washing with deionized water and drying at 45 °C for ∼10 h under vacuum condition.

Immobilization of Urease. The urease immobilization procedure was similar to that described in refs 24 and 25. A total of 0.2 g of glutaraldehyde linked AC granules were suspended in 50 mL of 0.5 mg/mL urease solution in a phosphate buffer (0.1 M, pH 7.2) and reacted in a shaking bed for 48 h at 4 °C. Finally, the AC-immobilized enzyme was separated by centrifuge and rinsed with a phosphate buffer (0.1 M, pH 7.2) and then with deionized water. The concentrations of enzyme were estimated from the absorbance at 275 nm. The amount of enzyme immobilized onto the support was calculated from the difference between initial and residual enzyme concentrations. Enzyme loading capacity was defined as the amount of bound urease per gram of support.[26]

Characterization. The surface oxygen-containing functional groups on the raw and oxidized ACs were quantitatively and qualitatively determined by Boehm titration. It depends on the amount and strength of the alkali reacted with the oxygen-containing groups. In the experiments, 0.2 g of the AC samples were separately added into four 100 mL conical flasks containing 20 mL of 0.02 M HCl, 0.02 M NaOH, 0.02 M $NaHCO_3$, and 0.02 M Na_2CO_3 solutions. The flasks were gently shaken for 48 h on a wrist shaker and then filtered. The filtrate was titrated with 0.02 M hydrochloric acid.

The Brunauer−Emmett−Teller (BET) surface area and average pore size of coconut shell AC-based samples were measured using TriStar 3000 from N_2 adsorption−desorption and Barrett−Joyner−Halenda (BJH) analysis. Fourier Transform infrared (FT-IR) spectra were recorded from KBr pellets using a Bruker Tensor27 spectrometer. X-ray photoelectron spectroscopy (XPS) analyses were conducted on an AXIS ULTRA^{DLD} spectrometer (Kratos) with achromatic Al(MONO) Kα X-radiation (1486.6 eV) as the X-ray source. The energy scale of the spectrometer was calibrated using copper, and the C1s binding energy of the graphitic peak was fixed at 284.6 eV for calibration.

Determination of Kinetic Parameters. A total of 0.2g of coconut shell AC-tethered urease was suspended in 6.0 mL of a 0.1 mol/L urea aqueous solution (0.1 M phosphate buffer, pH 6.0), and the mixture was incubated at 55 °C for 20 min. The reaction was terminated by adding 2 mL of a 10% trichloroacetic acid (TCA) solution. The absorbance of the solution was measured at 420 nm by p-dimethylaminobenzaldehyde colorimetry. The concentrations of urea were obtained from the urea calibration curve. The enzyme activity can be obtained from the following equation

$$\text{Urease activity (U/mg)} = (C_0 - C)V/tm$$

Here, V is the volume, C_0 is the initial concentration of urea, C is the final concentration of urea, t is the reaction time, and m denotes the mass of urease. For comparison, the same experimental procedures were followed to determine the activity of the free urease.[27] The maximum reaction rate (V_{max}) and the Michaelis−Menten constant (K_m) were determined by running a series of enzyme assays at varying substrate concentrations between 0.05 and 0.5 mol/L.

Determination of Optimum pH and Temperature. The activity versus temperature profiles of the free and immobilized urease were graphed on the basis of the activity values measured in a phosphate buffer of pH 7.0 at different temperatures in the range of 30−80 °C. The activity versus pH profiles were graphed measuring the activities at 60 °C in the pH range of 5.5−8.0. For the immobilized enzyme, 0.2 g of coconut shell AC-tethered urease was added to 6.0 mL of a 0.1 mol/L urea aqueous solution. To test the free enzyme, 1 mL of 1 mg/mL urease was mixed with 5.0 mL of a 0.1 mol/L urea aqueous solution. All reactions were run in a shaking bed for 20 min and repeated three times to achieve an average value in each case.

Degradation of Urea in a Packed Bed Reactor. Degradation of the urea aqueous solution (pH 7.2) was carried out over the immobilized urease in a packed bed. The packed column has an inner diameter of 1 cm and a length of 40 cm. One gram of coconut shell AC-tethered urease and 4 g of quartz granules were mixed and placed at the middle of the column with both ends filled with quartz granules. The conversion rate of urea can be calculate as follows

$$\text{Conversion rate}\ (\%) = \frac{C_0 - C}{C_0}(\times 100\%)$$

Also, C_0 is the inlet concentration of urea, and C is the outlet concentration of urea. The initial urea concentration was 0.1 mol/L. For all experiments, the reaction temperature was maintained at 70 °C. The concentrations of urea in reaction liquid were calculated as mentioned above.

RESULTS AND DISCUSSION

Functionalization of AC granules. The digital image of the raw AC granules is shown in Figure S1 of the Supporting Information. They have a specific surface area of 788.9 m^2/g and an average pore size of 3.39 nm. The pore distribution is shown in Figure S2a of the Supporting Information. After treatment by HNO_3, the specific surface area of AC was decreased to 706.8 m^2/g, and the average pore size was slightly increased to 3.41 nm. A possible explanation for this is that partial micropores in AC collapsed in the process of oxidation.

The Boehm titration is a commonly used technique to determine the surface oxygen-containing functional groups on carbon samples.[28−30] Total concentration of carboxylic and lactonic groups is 0.082 mmol g^{-1} for the raw AC. However, no phenolic group was detected by the titration. Oxidation by 20% HNO_3 generated a concentration of 0.330 mmol g^{-1} phenolic hydroxyl groups, and the total concentration of carboxylic and lactonic groups was increased to 0.262 mmol g^{-1}. The effect of different HNO_3 concentrations on surface chemistry was also investigated as shown in Table 1. The results show that the total concentration of the oxygen-containing functional groups increases with HNO_3 concentration, but the fraction of phenolic hydroxyl groups has a highest value of 55.8% at a concentration of 20% HNO_3. Excessive production of carboxylic and lactonic groups may result in collapse of the pore wall. Therefore, 20% HNO_3 is preferred to oxidize the AC.

Table 1. Contents of Oxygen-Containing Functional Groups on Raw and Oxidized ACs

concentrations of HNO_3 (wt %)	carboxylic and lactonic, (mmol/g)	phenolic (mmol/g)	fraction of phenolic groups (%)
0	0.082	–	–
5	0.137	–	–
20	0.262	0.330	55.8
40	0.625	0.402	39.1
60	1.027	0.391	27.6

XPS showed the main binding energy of the C1s electrons located at 284.9 eV, as shown in Figure 2, ascribed to graphitic carbons.[31−33] In addition, a small peak at 285.7 eV is assigned to the aliphatic carbons (C−COH or C−COO).[31−33] In the XPS spectra of both samples, the peak at 288.3 eV suggests the presence of some carbonate groups.[31−33] In contrast to the raw AC, the 20% HNO_3-treated AC displays a more intense peak at 286.8 eV, indicating oxidation of the partial carbon atoms to phenolic hydroxyl groups.[31−33] The area ratio of the peak at 286.8 eV to the peak at 284.9 eV was 0.176 for oxidized AC and 0.018 for raw AC as shown in Table S1 of the Supporting Information. The fractions of phenolic hydroxyl groups in the oxygen-containing groups were calculated based on the deconvoluted peak areas. They were 68.2% and 33.5% for the 20% HNO_3 treated AC and raw AC, respectively. XPS spectra of 5% HNO_3 and 60% HNO_3-treated AC are shown in Figure S3 of the Supporting Information. They quantitatively agree with the results observed by Boehm titration as well.

The effect of oxidation on the surface chemistry was also demonstrated by the FT-IR spectra. The FT-IR spectra of both raw and 20% HNO_3- treated AC are shown in Figure 3. In both cases, the spectra exhibited three characteristic IR bands. The band centered at 1405 cm^{-1} is assigned to the phenolic hydroxyl bending vibration, and the bands at 1062 and 1629 cm^{-1} correspond to the C−O stretching vibration of alcohol or ester and the C═O stretching vibration of carboxyl or ester,

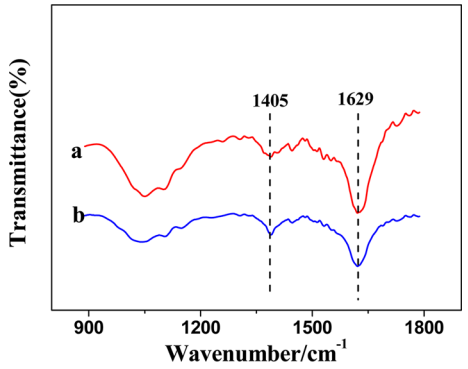

Figure 3. FT-IR spectra of (a) raw AC and (b) 20% HNO_3-oxidized AC.

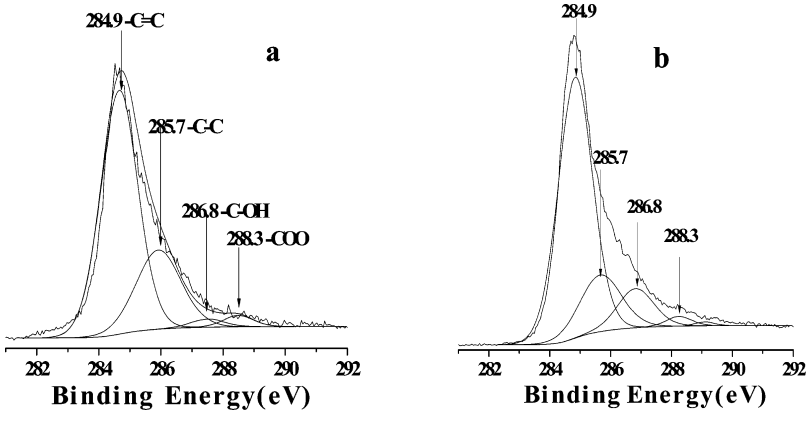

Figure 2. XPS spectra of (a) raw AC and (b) 20% HNO_3-treated AC.

dx.doi.org/10.1021/sc400335p | ACS Sustainable Chem. Eng. 2014, 2, 433−439

respectively.[34−37] In the IR spectrum of the oxidized AC as shown in Figure 3b, the relative intensity of 1405 or 1062 cm^{-1} was increased with respect to the band at 1629 cm^{-1}. Such an increase further suggests that new phenolic hydroxyl groups were generated due to HNO_3 oxidization. The FT-IR spectra of the AC treated at other concentrations of HNO_3 are shown in Figure S4 of the Supporting Information. The obtained results agree with the observations by XPS and Boehm titration.

The 20% HNO_3-treated AC granules were followed by reacting with aminosilane (APTMS) in toluene under nitrogen. The FT-IR spectra shown in Figure 4 revealed that the

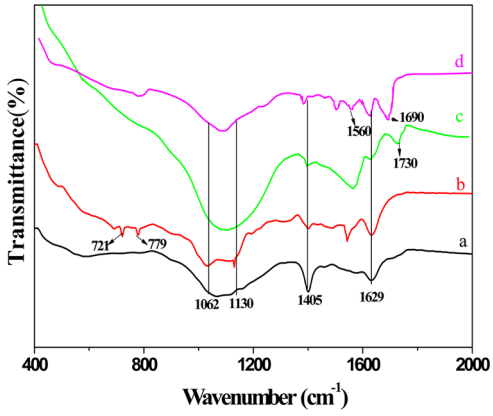

Figure 4. FT-IR spectra of (a) 20% HNO_3 oxidized AC, (b) aminosilylated AC, (c) glutaraldehyde-linked AC, and (d) AC-tethered urease.

aminosilane was grafted onto the oxidized AC. In contrast to the oxidized AC (Figure 4a), APTMS-grafted AC exhibited a weak band at 779 cm^{-1}, assigned to the stretching vibration of Ar−O−Si.[38] Meanwhile, it can be found that the phenolic hydroxyl band at 1405 cm^{-1} is significantly weakened as shown in Figure 4b. These indicated that APTMS effectively reacted with the phenolic hydroxyls. Furthermore, the bands at 721, 1130, and 1542 cm^{-1} are due to the stretching vibration of $-CH_2-$ units,[39] $C-NH_2$ stretching vibration, and N−H bending vibration in primary amine,[40,41] respectively. They are ascribed to the aminopropyl group of aminosilane. Successful grafting of APTMS was further corroborated by N_2 adsorption and desorption analysis. The specific surface area of the aminosilylated AC was apparently decreased to 538.9 from 706.8 m^2/g, and the average pore size was also decreased to 2.37 from 3.41 nm as shown in Figure S2c of the Supporting Information.

Aminosilylated AC was subjected to glutaraldehyde coupling prior to the enzyme immobilization reaction. The FT-IR spectrum in Figure 4c indicates that aldehydes are bonded onto the AC. An obvious evidence is the strong band at 1564 cm^{-1} assigned to the C═N double bond vibration.[38] Meanwhile, the NH_2 bending vibration peak of primary amine at 1542 cm^{-1} was significantly weakened,[40] indicating that the glutaraldehyde reacted with the primary amine of organosilane. The presence of the aldehyde groups on the AC was confirmed by the band at 1730 cm^{-1}, which is the stretching vibration of C═O at the other end of glutaraldehyde.[41] The band disappeared after immobilization of the urease as shown in Figure 4d. Instead, the bands ascribed to amide I and amide II of the urease were detected between 1500−1700 cm^{-1}.[42] Although it indicated that some urease was covalently attached onto the support through glutaraldehyde, it cannot be ruled out that some were immobilized via ionic exchange or hydrophobic adsorption.

Properties of Tethered Urease and Degradation of Urea. Urease loading capacity in the AC was 78.8 mg/g. Both the average pore size and surface area of the AC were decreased after enzyme immobilization. The nitrogen adsorption−desorption analysis shows that the BET surface area was decreased to 386.6 m^2/g, and the average pore size was narrowed down to 1.9 nm. Its pore size distribution is shown in Figure S2d of the Supporting Information. On the other hand, decrease in the average pore size suggests that urease was tethered into the pores and not merely onto the external surfaces.

Relative activities of both the tethered and free enzymes were investigated as a function of temperature as shown in Figure 5.

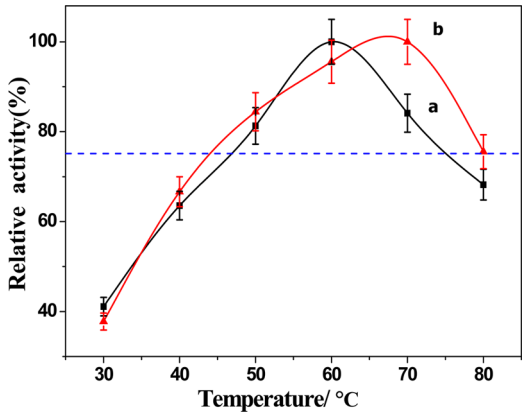

Figure 5. Effect of temperature on the activities of (a) free urease and (b) tethered ureases.

The optimum temperature was found to be 60 °C for free urease and 70 °C for tethered urease. The increase in the optimum temperature may be due to the improvement in the enzyme rigidity upon immobilization by covalent binding. Similar behavior has been observed in refs 26, 43, and 44. In terms of relative activity higher than 75% of the optimum activity, tethered urease shows a broader temperature range of 42−80 °C compared to 45−75 °C for the free enzyme. The effect of pH on the relative activity of urease was examined in the pH range of 5.5−8.0. As shown in Figure 6, an optimum enzyme activity was observed at pH 6.8 for free urease and pH 7.2 for tethered urease. Similar results have been previously

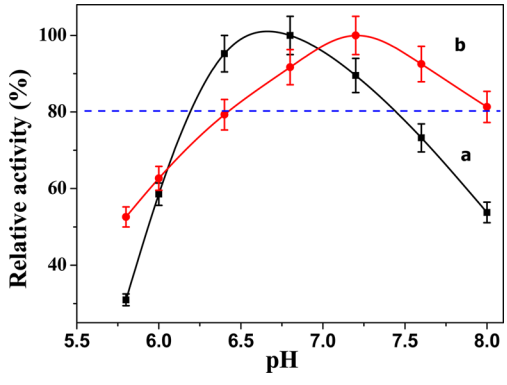

Figure 6. Effect of pH on the activities of (a) free urease and (b) tethered urease.

dx.doi.org/10.1021/sc400335p | ACS Sustainable Chem. Eng. 2014, 2, 433−439

reported in refs 45 and 46. The alkaline shift of maximum activity could be due to a higher H^+ concentration in the microenvironment of the support because lots of acidic groups were generated due to HNO_3 oxidation. However, the effect of the microenvironment of the support on the optimum pH is disputable.[47] Some researchers think strong interactions between enzyme and support will affect the intramolecular forces responsible for maintaining the conformation of the enzyme that would lead to a change in pH value.[48] The free enzyme had a pH range of 6.2−7.4, at which a relative activity was higher than 80%, while it occurred in a slightly widened pH range of 6.5−8.0 for the tethered enzyme. These results indicated that a very intense multipoint covalent attachment may occur in AC.[49] The formation of covalent bonds could attribute to a more rigid structure or the stabilization of the multimeric structure of the enzyme, which may limit the transition of enzyme conformation with a change in pH.[50]

The K_m values of the free and tethered ureases were 0.271 and 0.345 mol/L, respectively. The increase in K_m values was either due to the conformational changes of the enzyme, resulting in a lower possibility to form a substrate−enzyme complex, or to a lower accessibility of the substrate to the active sites of the immobilized enzyme caused by the increased diffusion limitation. Of course, the distortion generated by the enzyme support reaction may cause this phenomenon if the distortion is large enough.[5] For these reasons, the experimental results also show that the AC-tethered urease has a lower affinity to the reactant than the free urease. To our surprise, the AC tethered urease had a V_{max} value of 0.215 mol/min compared to 0.110 mol/min for the free urease. Many reports on immobilized ureases indicate a substantial decrease in V_{max}, such a different behavior might be attributed to a favorable change in enzyme structure upon immobilization and/or enhanced dissociation of the product/enzyme complex.[51]

Degradation of the urea aqueous solution was carried out over the AC-tethered urease in a packed bed reactor. A packed bed reactor has many favoring features, such as more convenience to separate the catalyst, ease of scale-up from a single tube to a pilot plant, and continuous operation for large-scale synthesis of chemicals under constant operating conditions.

First, various flow rates were tested as shown in Figure 7. It was found that urea can be completely degraded if the flow rate in the column was lower than 1.00 mL/min. Therefore, the flow rate was set to 1.00 mL/min (i.e., the residence time was 3 min) to study the effect of operation time on the relative activity as shown in Figure 8. The catalytic degradation had

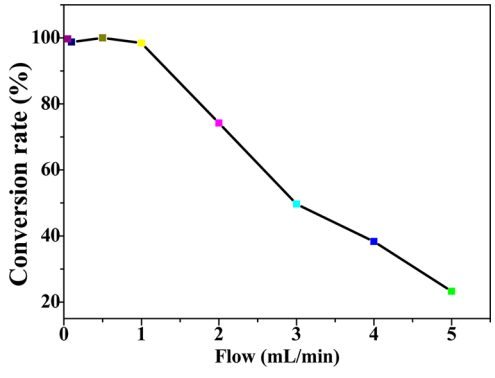

Figure 7. Effect of flow rate of urea aqueous solution on degradation of urea in a reactor packed with AC-tethered urease at 70 °C and pH 7.2.

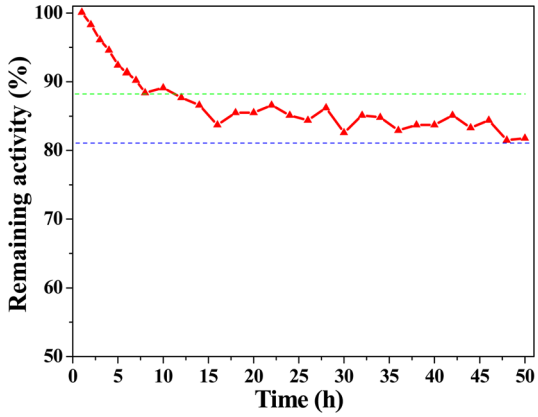

Figure 8. Plot of relative activity vs time for degradation of urea in a packed bed reactor on AC-tethered urease at 70 °C and pH 7.2. Residence time was 3 min.

proceeded for 50 h. It can be observed that the relative activity gradually decreased in the beginning 10 h, probably because some immobilized urease via ionic exchange or hydrophobic adsorption has a weak interaction with the support, and was easily flushed away by the continuous-flow reaction liquid. However, 10 h later, it was stabilized at 88% of the initial activity. The average activity retained ~84% in the following 40 h. In fact, the AC-tethered urease exhibited an extremely stable activity if one does not consider the influence from the lost of physically adsorbed urease. One gram of the AC-tethered urease degraded 3000 mL of 0.1 mol/L urea solution in 50 h, namely, 1 mg of urease degraded 3.06 mmol of urea.

Comparatively, Kara et al.[52] entrapped urease into chitosan−alginate polyelectrolyte complexes (C-A PEC) and P(AAm-co-AA)/carrageenan. A total of 0.5 g of C-A PEC-immobilized urease disposed a total of 20 mL of 0.2 M urea in a batch reactor after use 20 times and retained 55.0% of its original activity. Also, the retained activity was decreased to 80.0% for P(AAm-co-AA)/carrageenan-immobilized urease after the same operation.[52] Hidaka et al.[53]reported that the relative activity of the porous glass bead-immobilized alcohol oxidase was decreased to 57.3% after 20 h of running in a packed bed reactor. Wang et al.[54] immobilized catalase in mesoporous silica (MS) spheres by using a layer-by-layer assembly of multilayered composite thin shells. Catalase retained an activity of 70% after 25 successive batch reactions. Two commercial lipases (*Burkholderia cepacia* and *C. antarctica*) were encapsulated in silica aerogel. The reuse of these lipases allowed 11 cycles and kept only 60% of their initial activity in biodiesel synthesis by transesterification of sunflower seed oil with methyl acetate.[55]

CONCLUSIONS

Coconut shell AC-tethered urease has been successfully made by controlled oxidation to increase the content of phenolic hydroxyl groups. FT-IR and XPS results show that aminosilane was anchored onto the surface of AC. Both the BET surface area and average pore size were decreased after aminosilylation and enzyme immobilization. The tethered urease displayed an increased stability against the changes of temperature and pH in degradation of urea. The decrease in enzyme affinity may be due to the fact that some active sites of the enzyme were

covalently attached to AC, leading to partial inactivation. It also can be found that the tethered urease displayed a very stable catalytic activity for removal of urea in the packed bed. Moreover, the V_{max} value was enhanced after covalent immobilization in AC, which might be due to favorable change of the enzyme structure. This is also favorable for economical applications in medical and analytical fields.

■ ASSOCIATED CONTENT

Supporting Information

Figure S1: Digital image of the raw coconut shell AC granules. Figure S2: Pore distributions of the raw AC, oxidized AC, aminosilylated AC, and enzyme tethered AC. Table S1: Integral area percentage of C(1s) for the ACs treated with different HNO_3. Figure S3: XPS spectra of 5% HNO_3-treated AC and 60% HNO_3-treated AC. Figure S4: FT-IR spectra of the ACs treated with different concentrations of HNO_3 (0% HNO_3, 5% HNO_3, 40% HNO_3, and 60% HNO_3). This material is available free of charge via the Internet at http://pubs.acs.org.

■ AUTHOR INFORMATION

Corresponding Author

*Tel.: (86)-898-66279226. Fax: (86)-898-66271762. E-mail: bearcr_82@hotmail.com.

Notes

The authors declare no competing financial interest.

■ ACKNOWLEDGMENTS

The authors acknowledge the National Natural Science Foundation of China (Grant 21063006), Preferred Project of Chinese Ministry of Personnel for the Returned Overseas Chinese Scholars (excellent class), and the National Science and Technology Support Program (Grant 2012BAC18B02) for financing this work.

■ REFERENCES

(1) Krajewska, B. Ureases. II. Properties and their customizing by enzyme immobilizations: A review. *J. Mol. Catal. B: Enzym.* **2009**, *59* (1−3), 22−40.

(2) Lehmann, H. D.; Marten, R.; Gullberg, C. A. How to catch urea? Considerations on urea removal from hemofiltrate. *Artif. Organs* **1981**, *5* (3), 278−285.

(3) Krajewska, B.; Ureases, I. Functional, catalytic and kinetic properties: A review. *J. Mol. Catal. B: Enzym.* **2009**, *59* (3), 9−21.

(4) Li, S. J; Hu, J.; Liu, B. L. Use of chemically modified PMMA microspheres for enzyme immobilization. *BioSystems* **2004**, *77* (1−3), 25−32.

(5) Barbosa, O.; Torres, R.; Ortiz, C.; Berenguer-Murcia, A.; Rodrigues, R. C.; Fernandez-Lafuente, R. Heterofunctional supports in enzyme immobilization: From traditional immobilization protocols to opportunities in tuning enzyme properties. *Biomacromolecules* **2013**, *14* (8), 2433−2462.

(6) Magner, E. Immobilisation of enzymes on mesoporous silicate materials. *Chem. Soc. Rev.* **2013**, *42* (15), 6213−6222.

(7) Hwang, E. T.; Gu, M. B. Enzyme stabilization by nano/microsized hybrid materials. *Eng. Life Sci.* **2013**, *13* (1), 49−61.

(8) Lee, J. Y.; Shin, H. Y.; Kang, S. W.; Park, C.; Kim, S. W. Improvement of electrical properties via glucose oxidase-immobilization by actively turning over glucose for an enzyme-based biofuel cell modified with DNA-wrapped single walled nanotubes. *Biosens. Bioelectron.* **2010**, *26* (5), 2685−2688.

(9) Lee, J. Y.; Shin, H. Y.; Kang, S. W.; Park, C.; Kim, S. W. Use of bioelectrode containing DNA-wrapped single-walled carbon nanotubes for enzyme-based biofuel cell. *J. Power Sources.* **2010**, *195* (3), 750−755.

(10) Chae, H. J.; In, M. J.; Kim, E. Y. Optimization of protease immobilization by covalent binding using glutaraldehyde. *Appl. Biochem. Biotechnol.* **1998**, *73* (2−3), 195−204.

(11) Felipe, D.; Balkus, K. J., Jr. Enzyme immobilization in MCM-41 molecular sieve. *J. Mol. Catal. B: Enzym.* **1996**, *2* (2−3), 115−126.

(12) Zhang, X.; Guan, R. F.; Wu, D. Q.; Chan, K. Y. Enzyme immobilization on amino-functionalized mesostructured cellular foam surfaces, characterization and catalytic properties. *J. Mol. Catal. B: Enzym.* **2005**, *33* (1−2), 43−50.

(13) Yiu, H. P.; Wright, P. A.; Botting, N. P. Enzyme immobilisation using SBA-15 mesoporous molecular sieves with functionalised surfaces. *J. Mol. Catal. B: Enzym.* **2001**, *15* (1−3), 81−92.

(14) Takahashi, H.; Li, B.; Sasaki, T.; Miyazaki, C.; Kajino, T.; Inagaki, S. Immobilized enzymes in ordered mesoporous silica materials and improvement of their stability and catalytic activity in an organic solvent. *Microporous Mesoporous Mater.* **2001**, *44*−*45*, 755−763.

(15) Lie, K. L.; Lina, H. L. C.; Keng, T. W. Porous graphitic carbon shows promise for the rapid screening partial DPD deficiency in lymphocyte dihydropyrimidine dehydrogenase in Chinese, Indian and Malay in Singapore by using semi-automated HPLC-radioassay. *Clin. Biochem.* **2002**, *35* (1−3), 181−187.

(16) Macedo, J. S.; Otubo, L.; Ferreira, O. P.; Gimenez, I. F.; Mazali, I. O.; Barreto, L. S. Biomorphic activated porous carbons with complex microstructures from lignocellulosic residues. *Microporous Mesoporous Mater.* **2008**, *107* (3), 276−285.

(17) Kibarer, G. D.; Akovali, G. Optimization studies on the features of an activated charcoal-supported urease system. *Biomaterials* **1996**, *17*, 1473−1479.

(18) George, S.; Chellapandian, M.; Sivasankar, B.; Jayaraman, K. A new process for the treatment of fertilizer effluent using immobilized urease. *Bioprocess Eng.* **1997**, *16*, 83−85.

(19) Moynihan, H. J.; Lee, C. K.; Clark, W.; Wang, N. H. L. Urea hydrolysis by immobilized urease in a fixed-bed reactor: Analysis and kinetic parameter estimation. *Biotechnol. Bioeng.* **1989**, *34*, 951−963.

(20) Nakao, K.; Kiefner, A.; Furumoto, K.; Harada, T. Production of gluconic acid with immobilized glucose oxidase in airlift reactors. *Chem. Eng. Sci.* **1997**, *52*, 4127−4133.

(21) Webb, C.; Kang, H. K.; Moffat, G.; Williams, R. A.; Estevez, A. M.; Cuellar, J.; Jaraiz, E.; Galán, M. A. The magnetically stabilized fluidized bed bioreactor: A tool for improved mass transfer in immobilized enzyme systems? *J. Chem. Eng.* **1996**, *61* (3), 241−246.

(22) Hudson, S.; Cooney, J.; Magner, E. Proteins in mesoporous silicates. *Angew Chem., Int. Ed.* **2008**, *47* (45), 8582−8594.

(23) Zhang, Y.; Xiong, C. A new way to enhance the porosity and Y-faujasite percentage of in situ crystallized FCC catalyst. *Catal. Sci. Technol.* **2012**, *2* (3), 606−612.

(24) Dutta, S.; Bhattacharyya, A.; Ray, P.; Basu, S. Removal of mercury from its aqueous solution using charcoal-immobilized papain (CIP). *J. Hazard Mater.* **2009**, *172* (2−3), 888−896.

(25) Krishna, M. R. K.; William, E. L.; Thompson, M. Enhancement of the thermal and storage stability of urease by covalent attachment to phospholipid-bound silica. *Anal. Chem.* **1992**, *64* (9), 1062−1068.

(26) Kumar, A. G.; Swarnalatha, S.; Kamatchi, P.; Kirubagaran, R.; Perinmbam, K.; Sekaran, G. Immobilization of proteolytic enzyme on highly porous activated carbon derived from rice bran. *J. Porous Mater.* **2009**, *16* (4), 439−445.

(27) Kembhavi, A. A.; Kulkarni, A.; Pant, A. Salt-tolerant and thermal-stable alkaline protease from Bacillus subtilis NCIM. *Appl. Biochem. Biotechnol.* **1993**, *38* (1−2), 83−92.

(28) Kalijadis, A.; Vukcevic, M.; Jovanovic, Z.; Lausevic, Z. V.; Lausevic, M. Characterization of surface oxygen groups on different carbon materials by the Boehm method and temperature programmed desorption. *J. Serb. Chem Soc.* **2011**, *76* (5), 757−768.

(29) Oickle, A. M.; Goertzen, S. L.; Hopper, K. R.; Abdalla, Y. O.; Andreas, H. A. Standardization of the Boehm titration: Part II. Method of agitation, effect of filtering and dilute titrant. *Carbon* **2010**, *48* (12), 3313−3322.

(30) Salame, I. I.; Bandosz, T. J. Comparison of the surface features of two wood-based activated carbons. *Ind. Eng. Chem. Res.* **2000**, *39* (2), 301−306.
(31) Macias, G. A.; Valenzuela, C. C.; Gomez, S. V. Adsorption of Pb^{2+} by heat-treated and sulfurized activated carbon. *Carbon.* **1993**, *31*, 1249−1255.
(32) Biniak, S.; Szymanski, G.; Siedlewski, J.; Swiatkowski, A. The characterization of activated carbons with oxygen and nitrogen surface groups. *Carbon.* **1997**, *35*, 1799−1801.
(33) Polovina, M.; Babic, B.; Kaluderovic, B.; Dekanski, A. Surface characterization of oxidized activated carbon cloth. *Carbon.* **1997**, *35* (12), 1047−1052.
(34) Shin, S.; Jang, J.; Yoon, S. H.; Mochida, I.; Koretsky, G. M.; Knickelbein, M. B. A study on the effect of heat treatment on functional groups of pitch based activated carbon fiber using FTIR. *Carbon* **1997**, *35* (12), 1739−1743.
(35) Gomez, S. V.; Acedo, R. M.; Loper, P. A. J.; Peinado, A. J. L.; Calahorro, C. V. Oxidation of activated carbon by hydrogen peroxide. Study of surface functional groups by FTIR. *Fuel* **1994**, *73*, 387−395.
(36) Meldrum, B. J.; Rochester, C. H. *In situ* infrared study of the surface oxidation of activated carbon dispersed in potassium bromide. *J. Chem. Soc. Faraday Trans.* **1990**, *86*, 2997−3002.
(37) Meldrum, B. J.; Rochester, C. H. Fourier-transform infrared study of surface species on carbon mixed with KBr and reacted with CO_2, O_2 and CO. *J. Chem. Soc. Faraday Trans.* **1990**, *86*, 3647−3652.
(38) Xie, J. X. Application of Infrared spectrum in organic chemistry and pharmaceutical chemistry. *Beijing: Sci.Pre.* **2001**.
(39) Jagminas, A.; Kuzmarskye, J.; Niaura, G. Electrochemical formation and characterization of copper oxygenous compounds in alumina template from ethanolamine solutions. *Appl. Surf. Sci.* **2002**, *201* (1−4), 129−137.
(40) Shim, J. W.; Park, S. J.; Ryu, S. K. Effect of modification with HNO_3 and NaOH on metal adsorption by pitch-based activated carbon fibers. *Carbon.* **2001**, *39* (11), 1635−1642.
(41) Kang, Y.; He, J.; Guo, X. D.; Guo, X.; Song, Z. H. Influence of pore diameters on the immobilization of lipase in SBA-15. *Ind. Eng. Chem. Res.* **2007**, *46* (13), 4474−4479.
(42) Monier, M.; El-Sokkary, A. M. A. Modification and characterization of cellulosic cotton fibers for efficient immobilization of urease. *Int. J. Biol. Macromol.* **2012**, *51*, 18−24.
(43) Sedaghat, M. E.; Ghiaci, M.; Aghaei, H.; Soleimanian-Zad, S. Enzyme immobilization. Part 4. Immobilization of alkaline phosphatase on Na-sepiolite and modified sepiolite. *Appl. Clay Sci.* **2009**, *46* (2), 131−135.
(44) Peng, Y.; Wan, R. B.; Wang, X. P. Quantitative enzyme immobilization: Control of the carboxyl group density on support surface. *J. Mol. Catal. B: Enzym* **2009**, *61* (3−4), 296−302.
(45) Srinivasa, R. R.; Borkar, P. S.; Khobragade, C. N.; Sagar, A. D. Enzymatic activities of proteases immobilized on tri(4-formyl phenoxy) cyanurate. *Enzym Microb. Technol.* **2006**, *39* (4), 958−962.
(46) Sangeetha, K.; Abraham, T. E. Chemical modification of papain for use in alkaline medium. *J. Mol. Catal. B: Enzym.* **2006**, *38* (3−6), 171−177.
(47) Rodrigues, R. C.; Ortiz, C.; Berenguer-Murcia, A.; Torres, R.; Fernández-Lafuente, R. Modifying enzyme activity and selectivity by immobilization. *Chem.Soc.Rev.* **2013**, *42* (15), 6290−6307.
(48) Cengiz, S.; Çavaş, L.; Yurdakoç, K. Bentonite and sepioliteas supporting media: Immobilization of catalase. *Appl. Clay Sci.* **2012**, *65−66*, 114−120.
(49) Fernandez-Lafuente, R. Stabilization of multimeric enzymes: Strategies to prevent subunit dissociation. *Enzyme Microb. Technol.* **2009**, *45* (6−7), 405−418.
(50) Mohy, E. M. S.; Schroën, C. G. P. H.; Janssen, A. E. M.; Mita, D. G.; Tramper, J. Immobilization of penicillin G acylase onto chemically grafted nylon particles. *J. Mol. Catal. B: Enzym.* **2000**, *10* (4), 445−451.
(51) Azodi, M.; Falamaki, C.; Mohsenifar, A. Sucrose hydrolysis by invertase immobilized on functionalized porous silicon. *J. Mol. Catal. B: Enzym.* **2011**, *69*, 154−160.
(52) Kara, F.; Demirel, G. Ö.; Tümtürk, H. Application of chitosan-alginate polyelectrolyte complexes and interpenetrating polymer networks of poly (acrylamide-co-acrylic acid)/kappa-carrageenan as immobilization supports of enzyme. *Bioprocess Biosyst. Eng.* **2006**, *29*, 207−211.
(53) Hidaka, N.; Matsumoto, T. Gaseous ethanol oxidation by immobilized enzyme in a packed bed reactor. *Ind. Eng. Chem. Res.* **2000**, *39* (4), 909−915.
(54) Wang, Y. J.; Caruso, F. Mesoporous silica spheres as supports for enzyme immobilization and encapsulation. *Chem. Mater.* **2005**, *17* (5), 953−961.
(55) Orcaire, O.; Buisson, P.; Pierre, A. C. Application of silica aerogel encapsulated lipases in the synthesis of biodiesel by transesterification reactions. *J. Mol. Catal. B: Enzym* **2006**, *42* (3−4), 106−113.